HHS Public Access

Author manuscript

Nat Biotechnol. Author manuscript; available in PMC 2020 June 23.

Published in final edited form as:

Nat Biotechnol. 2020 February ; 38(2): 169–175. doi:10.1038/s41587-019-0357-y.

A reversible RNA on-switch that controls gene expression of AAV-delivered therapeutics *in vivo*

Guocai Zhong[1,3,*], **Haimin Wang**[1,3], **Wenhui He**[1], **Yujun Li**[2], **Huihui Mou**[1], **Zachary J. Tickner**[1], **Mai H. Tran**[1], **Tianling Ou**[1], **Yiming Yin**[1], **Huitian Diao**[1], **Michael Farzan**[1,*]

[1]Department of Immunology and Microbiology, The Scripps Research Institute, Jupiter, Florida, United States

[2]Department of Microbiology and Wu Lien-Teh Institute, Harbin Medical University, Harbin, China

[3]These authors contributed equally to this work

Abstract

Widespread use of gene therapy technologies is limited in part by the lack of small genetic switches with wide dynamic ranges that control transgene expression without the requirement of additional protein components[1–5]. Here, we engineered a class of type III hammerhead ribozymes to develop RNA switches that are highly efficient at *cis*-cleaving mammalian mRNAs and showed that they can be tightly regulated by a steric-blocking antisense oligonucleotide. Our variant ribozymes enable *in vivo* regulation of adeno-associated virus (AAV)-delivered transgenes, allowing dose-dependent control of protein expression up to 223-fold over at least 43 weeks. To test the potential of these reversible on-switches in gene therapy for anemia of chronic kidney disease[6], we demonstrate regulated expression of physiological levels of erythropoietin with a well-tolerated dose of the inducer oligonucleotide. These small, modular, and efficient RNA switches may improve the safety and efficacy, and broaden the use of gene therapies.

RNA-based switches[7–15] have two key strengths over protein-dependent transcriptional switches for gene-therapy applications. First, these switches are generally small (<200 bp), and thus can be easily incorporated into gene-therapy vectors with limited packaging capacity, for example those based on adeno-associated virus (AAV)[16]. Second, RNA switches do not require a potentially immunogenic non-self protein such as the rtTA protein for the Tet-On transcriptional activation system[5]. However, most RNA-based switches suffer from a narrow regulatory range, which usually precludes their use *in vivo*[10–14]. This narrow range can be a consequence of limited efficiency of the RNA effector domain or poor

*Correspondence to: zhonggc@szbl.ac.cn and mfarzan@scripps.edu.

Present address: G. Zhong, Translational Institute, Shenzhen Bay Laboratory, Shenzhen, China; G. Zhong, School of Chemical Biology and Biotechnology, Peking University Shenzhen Graduate School, Shenzhen, China; H. Wang, Translational Institute, Shenzhen Bay Laboratory, Shenzhen, China.

CONTRIBUTIONS

G.Z. conceived this project and developed it with M.F.. G.Z., H.W., W.H., Y.L., H.M., Z.T., M.T., T.O., Y.Y., and H.D. performed all experiments. G.Z. and M.F. wrote the manuscript.

COMPETING INTERESTS

G.Z. and M.F. are cofounders of Emmune Inc., a start-up company designing AAV-based treatments and prophylaxis for HIV-1.

response to the exogenous control agent. For example, hammerhead ribozymes, a class of small self-cleaving ribozymes with fast cleavage kinetics, are widely-used effector domains for RNA switches[7–13]. However, introduction of the most efficient of these ribozymes (N79, N117, and N107)[ref.9] at the 3′ UTR of a reporter gene affords only a 15- to 18-fold decrease in reporter expression relative to that observed with an inactive form of the same ribozyme in cell culture (Supplementary Fig. 1). This narrow dynamic range represents an upper theoretical bound on regulation using these ribozymes and is generally unsuitable for most *in vivo* applications.

To engineer RNA effector domains with wider dynamic ranges, we selected the modified *Schistosoma mansoni* hammerhead ribozyme, N107[ref.9], as a starting point. We rationally designed a panel of ribozyme variants, introduced them into the 3′ UTR of a *Gaussia* luciferase (Gluc) gene, and tested their catalytic activity in a reporter inhibition assay in cell culture (Fig. 1a). A functional ribozyme's catalytic activity was determined as its fold inhibition in Gluc expression relative to the expression observed with a corresponding catalytically inactive mutant. The N107 ribozyme, a type I hammerhead ribozyme[17], afforded only an 18-fold inhibition of Gluc expression in 293T cells (Fig. 1b). We reasoned that base-pairing interactions holding the long leaving strand of stem I and the tertiary interactions between this strand and loop II may result in a relatively slow disassembly of the cleaved type I ribozyme, allowing translation to continue and facilitating re-ligation of the cleaved substrate strand (Supplementary Figs. 1a and b). In contrast, a type III ribozyme can have a shorter leaving strand and fewer tertiary interactions between its leaving strand and the remainder of the ribozyme. Thus, type III ribozymes may disassemble more quickly after cleavage, preventing translation or re-ligation. Indeed, the ribozyme-mediated fold-inhibition of reporter expression significantly increased ($P = 3.3\times10^{-5}$) when N107 was converted to a type III ribozyme, T3H1, and placed at the 3′ UTR (Fig. 1b and Supplementary Figs. 1c-e). We then hypothesized that adjusting the stem-III annealing energy could accelerate disassembly without sacrificing cleavage efficiency (Supplementary Fig. 2a). Accordingly, we tested ribozyme variants with stem-III regions of varying lengths or with different potential inter-strand base stackings. Two of these stem-III variants, T3H16 and T3H29, inhibited Gluc expression in 293T cells by ~300-fold and outperformed all other stem-III variants tested (Fig. 1b and Supplementary Figs. 2b-h). When ribozyme activities of these stem-III variants were plotted against their calculated stem-III annealing energies[18], a peak of approximately −9 kcal/mol was observed, corresponding to the annealing energies of both T3H16 and T3H29 (Supplementary Fig. 2i). Tertiary interactions between loop II and a bulge on stem I enhanced hammerhead ribozyme activity by three orders of magnitude[19](Supplementary Fig. 3a). We therefore modified stem I of T3H16 to facilitate these tertiary interactions and improve ribozyme activity. We observed, as expected, that changes designed to destabilize the bulge I structure (T3H40 and T3H41) or directly impair these tertiary interactions (T3H54, T3H56, and T3H57) impaired ribozyme activity dramatically (Supplementary Figs. 3b-d). In contrast, changes that could stabilize the bulge I further improved the ribozyme activity to ~1000-fold (T3H44; Fig. 1b and Supplementary Fig. 3b). Finally, by changing the T3H44 loop I nucleotides to more stable tetraloops[20], ribozyme activity increased to ~1200-fold (Fig. 1b, and Supplementary Fig. 3e). Thus, by converting hammerhead ribozyme N107 to a type III ribozyme, and by optimizing its stem

III, stem I, and stem-I loop, ribozyme activity increased from 18- to ~1200-fold in 293T cells. The most efficient of these ribozymes, T3H48, was 60- to 80-fold more active than the type I ribozymes N107 and N117, and 92-fold more active than sTRSV ribozyme[21], a well-characterized type III ribozyme (Supplementary Figs. 3f-j). Sequences and secondary structures of the native *Schistosoma mansoni* ribozyme, N107, and key milestones in this optimization process are shown in Figure 1c. We further characterized these milestone ribozymes in four additional cell lines. Although some cell type-dependent variation in efficiency was observed, the order of ribozyme efficiency was unchanged across these cell lines, indicating these optimizations are not cell-type dependent (Supplementary Fig. 4a).

Ribozyme activity can be regulated by complementary phosphorodiamidate morpholino oligomers[9] (Fig. 2a). These morpholinos are a class of RNase H-independent antisense oligonucleotides that have been widely used to control splicing in scientific and clinical contexts, and have been approved for use in humans[22,23]. We first tested a panel of morpholinos complementary to different regions of T3H16 ribozyme for their ability to interfere with T3H16 self cleavage and thus induce gene expression. The M3 morpholino, which targets 5' portion of the stem I, most efficiently interfered with T3H16 placed at the 3' UTR of Gluc gene, inducing ~14-fold expression of Gluc in 293T cells, whereas the same morpholino had no effect on an inactive ribozyme control (Figs. 2b and c). We then tested an octa-guanidine dendrimer-coupled form[24] of M3 oligo, v-M3, with the 'v' denoting this dendrimer modification. v-M3 induced Gluc expression up to 200-fold in 293T cells, an effect that was dose dependent and markedly greater when T3H16 was placed at the 3′ UTR than at the 5′ UTR (Figs. 2d and e), consistent with the ability of morpholinos to inhibit translation when targeting the 5′ UTR[25]. We speculate that M3 best regulates T3H16 because it targets the 5′ region of the ribozyme, a region accessible during transcription before the ribozyme assembles. By contrast, morpholinos that target the 3′ region of the ribozyme must compete with the already synthesized 5′ strand. We accordingly assayed the ability of 5′-targeting morpholinos similar to M3 to regulate more efficient ribozyme variants (T3H38, T3H48) and a variant with a larger and more accessible stem-I loop (T3H52) (Fig. 2f). The most efficient regulation was afforded by v-M8, which specifically induced gene expression controlled by ribozyme T3H38 by ~300-fold in 293T cells (Fig. 2g and Supplementary Fig. 4b).

The exceptionally broad regulatory range of T3H38 by v-M8 suggested that this combination could provide useful *in vivo* control of an AAV transgene. We opted to assess this system in skeletal muscle because its slow turnover and extensive vascularization makes it a useful target tissue for gene therapies that express and secrete therapeutic proteins into the bloodstream to treat a range of human diseases [3,16,26–28]. Mouse gastrocnemius muscles were accordingly injected with an AAV1 vector expressing a firefly luciferase (Fluc) gene with the T3H38 ribozyme at its 3′ UTR (Fig. 3a). We observed efficient and dose-dependent induction of luciferase expression by the functional morpholino, v-M8, but not the control morpholino, v-NC (Figs. 3b and c, Supplementary Fig. 5a). Of note, intramuscular injection of morpholino only induced luciferase expression from the morpholino-injected hindlimb but not the opposite hindlimb. In addition, this locally induced expression was markedly more efficient than the expression induced by systemic injections of 25-fold higher morpholino dose (Fig. 3d and Supplementary Figs. 5b-d). Of note, v-M8 showed modest off-

target effect on several ubiquitously expressed genes (Supplementary Fig. 6). These data together indicate that local administration of morpholino for transgene regulation is more specific, more efficient, and safer for potential medical applications. Moreover, with local induction, luciferase expression could be repeatedly induced by more than 100-fold over a period of at least 43 weeks (Fig. 3e and Supplementary Fig. 7a). Reporter expression in these mice remained inducible even 20 months after AAV injection (Supplementary Fig. 7b). Liver is another attractive target organ for gene therapy[16]. Although the T3H38 ribozyme is similarly efficient in mouse liver and muscle tissue, we observed that our switch could regulate AAV-delivered transgene expression in liver by only 3-fold (Supplementary Figs. 7c-e). The higher regulatory range in muscle is likely a result of a higher effective concentration in muscle tissue when the morpholino is locally administered. More efficient regulation of liver expression may be achieved by replacing the octa-guanidine dendrimer in v-M8 with liver-targeting *N*-acetylgalactosamine[29]. Collectively, our data suggest a morpholino-regulated ribozyme-based on-switch is a feasible means of locally regulating expression of secreted biologics from muscle tissue.

To highlight one medically useful application of this system, we sought to control the expression of AAV-delivered erythropoietin (Epo), a commonly administered biologic for the treatment of anemia associated with chronic kidney disease[6,30]. Mouse gastrocnemius muscles were injected with an AAV1 vector delivering the murine Epo gene with the T3H38 ribozyme at its 3′ UTR (Fig. 4a). The v-M8 morpholino was administered twelve days later to the same site. v-M8 induced Epo expression and hematocrit levels to those observed with an Epo transgene incorporating a catalytically inactive T3H38 (Fig. 4b). Epo concentrations remained elevated over at least two weeks with an induction half-life of 122 hours. In contrast, the half-life of recombinant Epo protein was ~3 hours, consistent with previous studies[31]. Morpholino-induced Epo peaked at 15,000 pg/ml, 100-fold higher than physiological concentrations, and far higher than what would be optimal for Epo treatment[32]. We thus injected mice intramuscularly with lower doses of AAV (5×10^9 and 2×10^9 genome copies) and also varied the dose of morpholino (0, 0.1, 0.5 and 2.5 mg/kg). We observed morpholino- as well as AAV-dose-dependent induction of erythropoietin expression and hematocrit elevation (Figs. 4c-f and Supplementary Fig. 8). When mice were injected with 5×10^9 genome copies of AAV, the lowest tested dose of morpholino (0.1 mg/kg) induced Epo expression at close-to-physiological concentrations for over a week (Fig. 4c and Supplementary Fig. 8a). When the AAV dose was further lowered to 2×10^9 genome copies, morpholino-induced Epo expression peaked at only 110 pg/ml, a concentration lower than physiological levels, but induced hematocrit remained elevated for more than 4 weeks (Figs. 4e and f, Supplementary Fig. 8b), reflecting the sensitivity of hemocrit values to low Epo levels and the extended life-span of red blood cells. Figures 4g and h summarize Epo induction values in response to different doses of morpholino and AAV, respectively. Thus, sustained expression of physiologically relevant levels of Epo can be induced from a T3H38 ribozyme-regulated AAV transgene by administration of 0.1–0.5 mg/kg morpholino. These doses of v-M8 morpholino are 25- to 125-fold lower than the tested highest tolerable dose of v-M8 in mice (12.5 mg/kg; Supplementary Fig. 9).

Gene therapy has begun to provide impressive therapeutic benefits and potential cures for a range of human diseases, including inherited genetic diseases, cancers, and infectious

diseases[16,33]. Most of these applications use an AAV vector to express a therapeutic protein, an approach favored due to the safety of these vectors and their relatively lower immunogenicity[15]. RNA-based switches, with their small size and lack of dependence on exogenous proteins, make ideal regulators of AAV transgenes, but their narrow regulatory ranges preclude their *in vivo* use[10–14]. A single exception to this is an on-switch system built from an engineered hammerhead ribozyme similar to N107, but regulation of this system is mediated by a compound that disrupts ribozyme function by directly incorporating a nucleoside analogue into the transgene mRNA[9,34], and thus would not be suitable for clinical applications.

Here we increased the dynamic range of a hammerhead ribozyme and combined it with an optimized morpholino to develop an on-switch system efficient enough for *in vivo* use. Specifically, we observed in mice an approximately 200-fold induction of an AAV-expressed biologic, comparable to regulation mediated by exogenous transcription factors[3,35]. Moreover, the dose of AAV vectors used here, 5×10^9 genome copies per mouse, is 5 to 40 fold lower than what was used to achieve similar expression with transcriptional regulatory switches[3,35], highlighting both the safety and cost-effectiveness of the system developed here. Notably, morpholinos have the potential to be safe in humans, and indeed a morpholino has been approved for human use for doses up to 50 mg/kg weekly infused systemically[23]. We show that morpholino concentration of 0.1 mg/kg administered locally can induce physiological levels of Epo (Fig. 4c and Supplementary Fig. 8a), suggesting that this inducible system may be safe enough for human use.

Epo-deficient anemia contributes substantially to morbidity and mortality among chronic kidney disease patients, and recombinant Epo protein is the standard of care for this condition[6,30]. However, elevated risk of cardiovascular complications and death are thought associated with the high C_{max} of plasma Epo after administration of recombinant protein[32,36]. Due to its short half-life, the C_{max} of recombinant Epo necessary to maintain therapeutic levels typically requires initial concentrations 6- to 60-fold over physiological Epo concentrations[6,37]. In this study, a single administration of morpholino at a well-tolerated dose induced physiological levels of Epo with an induction half-life ~40-times that of passively administered Epo proteins (Figs. 4b and g). Thus, a tightly regulated AAV-based Epo expression system such as that demonstrated here could circumvent safety concerns associated with the current standard of care. Moreover, the absence of exogenous regulatory proteins, and the ability to delay transgene expression until well after AAV-induced innate responses subside, may prevent the emergence of anti-transgene antibodies observed with other AAV-based systems[38,39]. The expression of Epo from human tissue may also obviate immune responses observed with Epo manufactured in non-human cell lines[40].

The utility of the reversible on-switch developed here extends beyond Epo expression. The size of the regulatory element is 63 bp, small enough, for example, to control expression of a CRISPR effector protein and guide RNA in the same AAV vector, minimizing off-target activity and immunogenicity in therapeutic settings. Moreover, roughly half of unregulated transgene expression can be recovered. It is therefore useful in contexts, such as therapeutic antibodies, where high expression is paramount. The system is promoter-independent, allowing tissue-specific induction. Local administration and induction allow for independent

regulation of two or more therapeutics in the same individual. As shown, morpholino induction can last for weeks, improving the half-lives of short-lived proteins or peptides. Finally, some of these properties may be useful for regulating survival, payload expression, or local activation of cell-based gene therapies[33].

METHODS

Plasmids

DNA fragments encoding ribozyme variants were synthesized by Integrated DNA Technologies (IDT). Dual-reporter plasmids encoding a ribozyme-regulated Gaussia luciferase (Gluc) gene and an unregulated *Cypridina* luciferase (Cluc) gene were constructed by cloning a Gluc gene fragment and a ribozyme-encoding DNA fragment into the pCMV-CLuc2 (New England Biolabs) between *Xma*I and *Bst*BI restriction sites. AAV vector plasmids encoding firefly luciferase (Fluc) reporter were constructed by cloning a Fluc gene fragment and a T3H38 ribozyme-encoding DNA fragment into the pAAV-MCS plasmid (Agilent Technologies) between *Eco*RI and *Xho*I restriction sites. AAV vector plasmids encoding the mouse erythropoietin (Epo) transgene were constructed by cloning a CASI promoter[27], a mouse Epo gene fragment, and a T3H38 ribozyme-encoding DNA fragment into the pAAV-MCS plasmid (Agilent Technologies) between *Mlu*I and *Xho*I restriction sites.

Cell culture

All the cell lines were maintained in Dulbecco's Modified Eagle Medium (DMEM, Life Technologies) at 37°C in a 5% CO_2-humidified incubator. All growth media were supplemented with 2 mM Glutamax-I™ (Life Technologies), 100 μM non-essential amino acids (Life Technologies), 100 U/mL penicillin and 100 μg/mL streptomycin (Life Technologies), and 10% FBS (Hyclone). Cell lines from ATCC (293T, HeLa, MEF, and A549) were confirmed mycoplasma-free by the provider.

Measurement of ribozyme-regulated gene expression in transiently transfected cells

Cells seeded in polylysine pre-treated 48-well plate with antibiotic-free growth medium were transfected with 25 ng of the ribozyme-regulated Gluc expression plasmids using 0.3 μL Lipofectamine 2000 (Life Technologies) for three to five hours. Expression of Gluc and Cluc reporters was measured one day post transfection. A functional ribozyme's activity was calculated as 'fold' inhibition in the Gluc expression relative to the inactive ribozyme control. Cluc was used as a reference reporter for plasmid dose and transfection efficiency.

Measurement of unmodified morpholino-induced gene expression in transiently transfected cells

Cells seeded in polylysine pre-treated 48-well plate with antibiotic-free growth medium were transfected with 25 ng of the ribozyme-regulated Gluc expression plasmids using 0.3 μL Lipofectamine 2000 (Life Technologies) for three to five hours. Cell culture medium was then changed with fresh medium. After additional two hours, cells were treated overnight with 10 μM unmodified morpholino (synthesized by Gene Tools) and 1.2 μL Endo-Porter delivery reagent (Gene Tools) in 200 μL culture medium. Expression of Gluc and Cluc

reporters was measured one day post transfection. A functional morpholino's activity was calculated as fold induction in the Gluc reporter expression relative to the Gluc expression from control morpholino-treated cells. Cluc was used as a reference reporter for plasmid dose and transfection efficiency.

Measurement of octa-guanidine dendrimer-coupled morpholino-induced gene expression in transiently transfected cells

Cells seeded in polylysine pre-treated 48-well plate with antibiotic-free growth medium were first incubated overnight with 10 μM morpholino (synthesized by Gene Tools) in 200 μL culture medium. Cell culture medium was then changed with fresh medium. After additional three hours, cells were transfected with 25 ng of the ribozyme-regulated Gluc expression plasmids using 0.3 μL Lipofectamine 2000 (Life Technologies) for three to five hours. Expression of Gluc and Cluc reporters was measured on day one or two post transfection. A functional morpholino's activity was calculated as fold induction in the Gluc reporter expression relative to the Gluc expression from control morpholino-treated cells. Cluc was used as a reference reporter for plasmid dose and transfection efficiency.

Gluc and Cluc luminescence flash assays

To measure Gluc expression, 20 μL of cell culture supernatant of each sample and 100 μL of assay buffer containing 4 μM coelenterazine native (Biosynth Chemistry & Biology) were added to one well of a 96-well white opaque assay plate (Corning), and measured with the Centro LB 960 microplate luminometer (Berthold Technologies) for 0.5 second/well. Cluc expression was measured using Pierce *Cypridina* Luciferase Flash Assay Kit (Thermo Scientific Pierce) following the manufacturer's instructions. In brief, 20 μL of cell culture supernatant of each sample and 50 μL of Cluc assay buffer (*Cypridina* Flash Assay Buffer + Vargulin) were added to one well of a 96-well black opaque assay plate (Corning), and measured with the Centro LB 960 microplate luminometer for 0.1 second/well.

Production of adeno-associated virus (AAV) vectors

293T cells plated at 70% confluence in 150 mm cell culture dishes (Corning) were transfected using PEI MAX 40K Linear (Polysciences) with 13 μg of plasmid encoding AAV replication and capsid proteins, 13 μg of plasmid encoding helper proteins, and 13 μg of pAAV-MCS-based plasmids encoding ribozyme-regulated Fluc, or mouse Epo. Sixty to seventy-two hours post-transfection, cells were harvested for AAV particle purification using All-Serotype AAVpro Purification Kit (Takara). Purified AAV particles were concentrated in PBS to ~1×10^{13} genome copies/ml. Titers of the particles were determined by quantitative PCR using AAVpro Titration Kit Ver.2 (Takara).

Mouse AAV experiments

Six-week-old male or 8-week-old female BALB/c mice (Charles River Laboratories, or The Jackson Laboratory) were randomly separated into age-matched groups without blinding. For muscle transduction experiments, mice were intramuscularly (i.m.) injected in the gastrocnemius muscles with 20 μL of purified AAV1 particles (0.2, 0.5, or 1×10^{10} genome copies per mice) carrying firefly luciferase (Fluc) or mouse Epo gene regulated by active or

inactive T3H38 ribozyme. For liver transduction experiments, mice were intravenously (i.v.) injected with 100 μL of purified AAV8 particles (1×10^{10} genome copies per mice) carrying Fluc gene regulated by an active or an inactive T3H38 ribozyme. At different time points post AAV injection, as shown in each figure, mice were either i.m. injected at the same AAV-injection site with 0.1, 0.5 or 2.5 mg/kg of octa-guanidine dendrimer-coupled control (v-NC) or v-M8 morpholino in 40 μL PBS, or i.v. injected with 12.5 mg/kg of v-M8 in 100 μL PBS. As a control experiment for AAV-delivered mouse Epo, a group of 4 mice received no AAV were intraperitoneally (i.p.) injected with 3 μg of recombinant mouse Epo protein (BioLegend) in 100 μL PBS. Mice injected with AAV-Fluc were subjected to *in vivo* bioluminescence imaging to quantify Fluc expression at the indicated time points. Mice injected with AAV-Epo were subjected to blood sample collection and measurements of hematocrit counts and plasma Epo concentration at the indicated time points. All mice studies were performed in accordance with the Scripps Florida Institutional Animal Care and Use Committee animal use protocol number 17–026.

In vivo Fluc bioluminescent imaging

Prior to imaging, the mice were i.p. injected with 100 μL of 30 mg/ml RediJect D-Luciferin Ultra bioluminescent substrate (PerkinElmer). Mice were then anesthetized with isoflurane and imaged within 20 minutes for bioluminescence using the *in vivo* imager. All the bioluminescence data, except for those shown in Supplementary Figures 7d and e, were collected using the IVIS Spectrum *In Vivo* Imaging System (PerkinElmer), and bioluminescent photon outputs were quantified using the Living Image Software (PerkinElmer). The bioluminescence data shown in Supplementary Figures 7d and e were collected using the Lago X optical imaging system (Spectral Instruments Imaging) and analyzed using Aura software (Spectral Instruments Imaging).

Measuring hematocrit counts and plasma Epo concentration

At each indicated time point in Figure 4, 27 μL of blood sample was collected from tail vein of each mouse and mixed immediately with 3 μL of 0.2M EDTA. The blood samples were then drawn into heparin-treated microhematocrit capillary tubes (Fisher Scientific) and centrifuged at 16,000 g for 3 min at 4°C using a micro-hematocrit centrifuge (Thermo Scientific). Hematocrit counts were then measured with a Critocaps micro-hematocrit tube reader (Leica Microsystems Inc). Then plasma samples in the capillary tubes were collected and stored at −80°C. Twenty-fold diluted plasma samples were then used for measuring plasma Epo protein concentration using Mouse Erythropoietin Quantikine ELISA Kit (R&D), and ELISA samples were measured with Victor X3 multi-label plate reader (PerkinElmer). Paired sample Student's *t*-tests were performed to analyze the statistical significance of the plasma Epo concentration and hematocrit count differences among different treatment groups.

v-M8 morpholino off-target analysis

Total RNA samples were first prepared from morpholino-treated 293T cells using Trizol reagent (Life Technologies), and then treated with amplification grade DNase I (Thermo Fisher Scientific). Then 100–300 ng total RNA and a pair of 11 PCR-validated transcript-specific primers were subjected to a RT-qPCR reaction using Luna Universal One-Step RT-

qPCR kit (New England BioLabs) and Eco Real-Time PCR system (Illumina). Relative quantification of each potential off-target transcript was performed using GAPDH as an internal control.

v-M8 morpholino *in vivo* dose tolerance test

Nineteen- or eight-week old female BALB/c mice (The Jackson Laboratory) were i.v. injected with v-M8 morpholino at 0, 2.5, 5.0, 10.0, or 12.5 mg/kg/day for two days or four days. Mice body weights were measured at the indicated time points. All mice studies were performed in accordance with the Scripps Florida Institutional Animal Care and Use Committee animal use protocol number 17–026.

Statistical analysis

Data expressed as mean values ± s.d. or s.e.m. Statistical analyses were performed using one-sided paired-sample or two-sample Student's *t*-test using GraphPad Prism 6.0 software when applicable. Differences were considered significant at $P < 0.01$ or $P < 0.05$ as indicated.

Life Science Reporting Summary

Further information on experimental design and reagents is available in the Nature Research Reporting Summary linked to this article.

Data availability

Our research resources, including methods, plasmids, and protocols, are available upon reasonable request to qualified academic investigators for noncommercial research purposes. All reagents developed, such as vector plasmids, as well as detailed methods, will be made available upon written request. The corresponding author adheres to the NIH Grants Policy on Sharing of Unique Research Resources including the "Sharing of Biomedical Research Resources: Principles and Guidelines for Recipients of NIH Grants and Contracts."

Supplementary Material

Refer to Web version on PubMed Central for supplementary material.

ACKNOWLEGEMENTS

This work is supported by NIH R37 AI091476, NIH AI1129868, and NIH DP1 DA043912 (M.Farzan).

REFERENCES

1. Black JB, Perez-Pinera P & Gersbach CA Mammalian Synthetic Biology: Engineering Biological Systems. Annu Rev Biomed Eng 19, 249–277, (2017). [PubMed: 28633563]
2. Alexander HK et al. Selected technologies to control genes and their products for experimental and clinical purposes. Arch Immunol Ther Exp (Warsz) 55, 139–149, (2007). [PubMed: 17557142]
3. Ye X et al. Regulated delivery of therapeutic proteins after in vivo somatic cell gene transfer. Science 283, 88–91, (1999). [PubMed: 9872748]
4. Hjelm BE et al. Mifepristone-inducible transgene expression in neural progenitor cells in vitro and in vivo. Gene Ther 23, 424–437, (2016). [PubMed: 26863047]

5. Favre D et al. Lack of an immune response against the tetracycline-dependent transactivator correlates with long-term doxycycline-regulated transgene expression in nonhuman primates after intramuscular injection of recombinant adeno-associated virus. J Virol 76, 11605–11611, (2002). [PubMed: 12388721]
6. Hayat A, Haria D & Salifu MO Erythropoietin stimulating agents in the management of anemia of chronic kidney disease. Patient Prefer Adherence 2, 195–200, (2008). [PubMed: 19920963]
7. Auslander S & Fussenegger M Synthetic RNA-based switches for mammalian gene expression control. Curr Opin Biotechnol 48, 54–60, (2017). [PubMed: 28388465]
8. Tang J & Breaker RR Rational design of allosteric ribozymes. Chem Biol 4, 453–459, (1997). [PubMed: 9224568]
9. Yen L et al. Exogenous control of mammalian gene expression through modulation of RNA self-cleavage. Nature 431, 471–476, (2004). [PubMed: 15386015]
10. Win MN & Smolke CD A modular and extensible RNA-based gene-regulatory platform for engineering cellular function. Proc Natl Acad Sci U S A 104, 14283–14288, (2007). [PubMed: 17709748]
11. Ketzer P, Haas SF, Engelhardt S, Hartig JS & Nettelbeck DM Synthetic riboswitches for external regulation of genes transferred by replication-deficient and oncolytic adenoviruses. Nucleic Acids Res 40, e167, (2012). [PubMed: 22885302]
12. Beilstein K, Wittmann A, Grez M & Suess B Conditional control of mammalian gene expression by tetracycline-dependent hammerhead ribozymes. ACS Synth Biol 4, 526–534, (2015). [PubMed: 25265236]
13. Zhong G, Wang H, Bailey CC, Gao G & Farzan M Rational design of aptazyme riboswitches for efficient control of gene expression in mammalian cells. Elife 5, e18858, (2016). [PubMed: 27805569]
14. Mou H et al. Conditional Regulation of Gene Expression by Ligand-Induced Occlusion of a MicroRNA Target Sequence. Mol Ther 26, 1277–1286, (2018). [PubMed: 29567311]
15. Wroblewska L et al. Mammalian synthetic circuits with RNA binding proteins for RNA-only delivery. Nat Biotechnol 33, 839–841, (2015). [PubMed: 26237515]
16. Wang D, Tai PWL & Gao G Adeno-associated virus vector as a platform for gene therapy delivery. Nat Rev Drug Discov 18, 358–378, (2019). [PubMed: 30710128]
17. Scott WG, Horan LH & Martick M The hammerhead ribozyme: structure, catalysis, and gene regulation. Prog Mol Biol Transl Sci 120, 1–23, (2013). [PubMed: 24156940]
18. Bellaousov S, Reuter JS, Seetin MG & Mathews DH RNAstructure: Web servers for RNA secondary structure prediction and analysis. Nucleic Acids Res 41, W471–474, (2013). [PubMed: 23620284]
19. Martick M & Scott WG Tertiary contacts distant from the active site prime a ribozyme for catalysis. Cell 126, 309–320, (2006). [PubMed: 16859740]
20. Bottaro S & Lindorff-Larsen K Mapping the Universe of RNA Tetraloop Folds. Biophysical journal 113, 257–267, (2017). [PubMed: 28673616]
21. Chi YI et al. Capturing hammerhead ribozyme structures in action by modulating general base catalysis. PLoS Biol 6, e234, (2008). [PubMed: 18834200]
22. Summerton JE Morpholino, siRNA, and S-DNA compared: impact of structure and mechanism of action on off-target effects and sequence specificity. Curr Top Med Chem 7, 651–660, (2007). [PubMed: 17430206]
23. Stein CA & Castanotto D FDA-Approved Oligonucleotide Therapies in 2017. Mol Ther 25, 1069–1075, (2017). [PubMed: 28366767]
24. Morcos PA, Li Y & Jiang S Vivo-Morpholinos: a non-peptide transporter delivers Morpholinos into a wide array of mouse tissues. Biotechniques 45, 613–614, 616, 618 passim, (2008). [PubMed: 19238792]
25. Summerton J Morpholino antisense oligomers: the case for an RNase H-independent structural type. Biochim Biophys Acta 1489, 141–158, (1999). [PubMed: 10807004]
26. Rivera VM et al. Long-term regulated expression of growth hormone in mice after intramuscular gene transfer. Proc Natl Acad Sci U S A 96, 8657–8662, (1999). [PubMed: 10411931]

27. Balazs AB et al. Antibody-based protection against HIV infection by vectored immunoprophylaxis. Nature 481, 81–84, (2012).
28. Gardner MR et al. AAV-expressed eCD4-Ig provides durable protection from multiple SHIV challenges. Nature 519, 87–91, (2015). [PubMed: 25707797]
29. Huang Y Preclinical and Clinical Advances of GalNAc-Decorated Nucleic Acid Therapeutics. Mol Ther Nucleic Acids 6, 116–132, (2017). [PubMed: 28325278]
30. Adamson JW & Eschbach JW Erythropoietin for end-stage renal disease. N Engl J Med 339, 625–627, (1998). [PubMed: 9718384]
31. Lee DE, Son W, Ha BJ, Oh MS & Yoo OJ The prolonged half-lives of new erythropoietin derivatives via peptide addition. Biochem Biophys Res Commun 339, 380–385, (2006). [PubMed: 16314154]
32. Koulouridis I, Alfayez M, Trikalinos TA, Balk EM & Jaber BL Dose of erythropoiesis-stimulating agents and adverse outcomes in CKD: a metaregression analysis. Am J Kidney Dis 61, 44–56, (2013). [PubMed: 22921639]
33. Dunbar CE et al. Gene therapy comes of age. Science 359, eaan4672, (2018). [PubMed: 29326244]
34. Yen L, Magnier M, Weissleder R, Stockwell BR & Mulligan RC Identification of inhibitors of ribozyme self-cleavage in mammalian cells via high-throughput screening of chemical libraries. RNA 12, 797–806, (2006). [PubMed: 16556935]
35. Bohl D, Salvetti A, Moullier P & Heard JM Control of erythropoietin delivery by doxycycline in mice after intramuscular injection of adeno-associated vector. Blood 92, 1512–1517, (1998). [PubMed: 9716577]
36. Blum S et al. TARGT Gene Therapy Platform for Correction of Anemia in End-Stage Renal Disease. N Engl J Med 376, 189–191, (2017). [PubMed: 28076704]
37. Macdougall IC et al. Pharmacokinetics of novel erythropoiesis stimulating protein compared with epoetin alfa in dialysis patients. J Am Soc Nephrol 10, 2392–2395, (1999). [PubMed: 10541299]
38. Chenuaud P et al. Autoimmune anemia in macaques following erythropoietin gene therapy. Blood 103, 3303–3304, (2004). [PubMed: 14739218]
39. Gao G et al. Erythropoietin gene therapy leads to autoimmune anemia in macaques. Blood 103, 3300–3302, (2004). [PubMed: 14695227]
40. Bunn HF Drug-induced autoimmune red-cell aplasia. N Engl J Med 346, 522–523, (2002). [PubMed: 11844855]

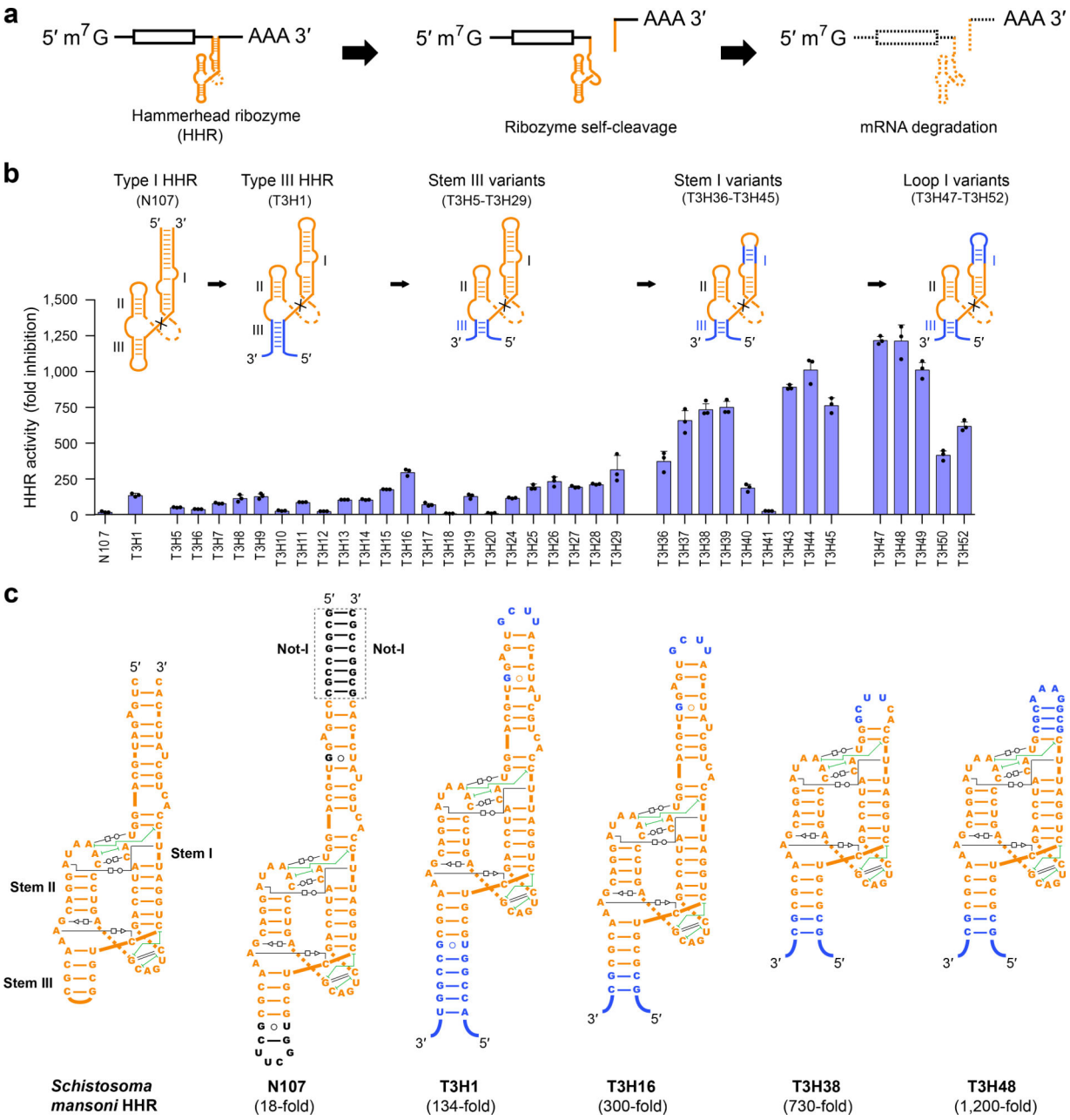

Figure 1. Development of a class of highly efficient hammerhead ribozymes (HHR).

(**a**) A diagram representing HHR-mediated inactivation of gene expression. (**b**) A panel of engineered HHR variants were tested in a reporter assay in which an expression vector encoding *Gaussia* luciferase (Gluc) and *Cypridina* luciferase (Cluc), each driven by an independent promoter, was used. A catalytically active ribozyme variant was placed to the 3′ UTR of the Gluc gene, and compared with a catalytically inactive form of the same ribozyme. Reporter plasmids were transfected into 293T cells, and the functional ribozyme's activity was calculated as fold inhibition in the Gluc expression relative to the inactive ribozyme control. Cluc activity was simultaneously monitored to control for dose and transfection efficiencies. As shown, the catalytic activity of the previously described

Schistosoma mansoni HHR variant, N107, was improved from its original 18-fold to 1,200-fold (blue bars) through a series of modifications, as represented above the figure. These include conversion of the type I HHR N107 to a type III HHR, optimization of stem III of the resulting type III ribozymes, modification of stem I to stabilize the tertiary interactions essential for ribozyme function, and alteration of loop I to facilitate hairpin formation. Data shown are representative of three independent experiments with similar results, and data points represent mean ± s.d. of three cell cultures. (**c**) Sequences and secondary structures of a natural *Schistosoma mansoni* HHR, the N107 ribozyme, and milestone type III ribozyme variants characterized in panel b. Differences between the native *Schistosoma mansoni* ribozyme and N107 are indicated in black. Successive modifications from N107 are indicated in blue. Further details are provided in the legend of Supplementary Figure 1.

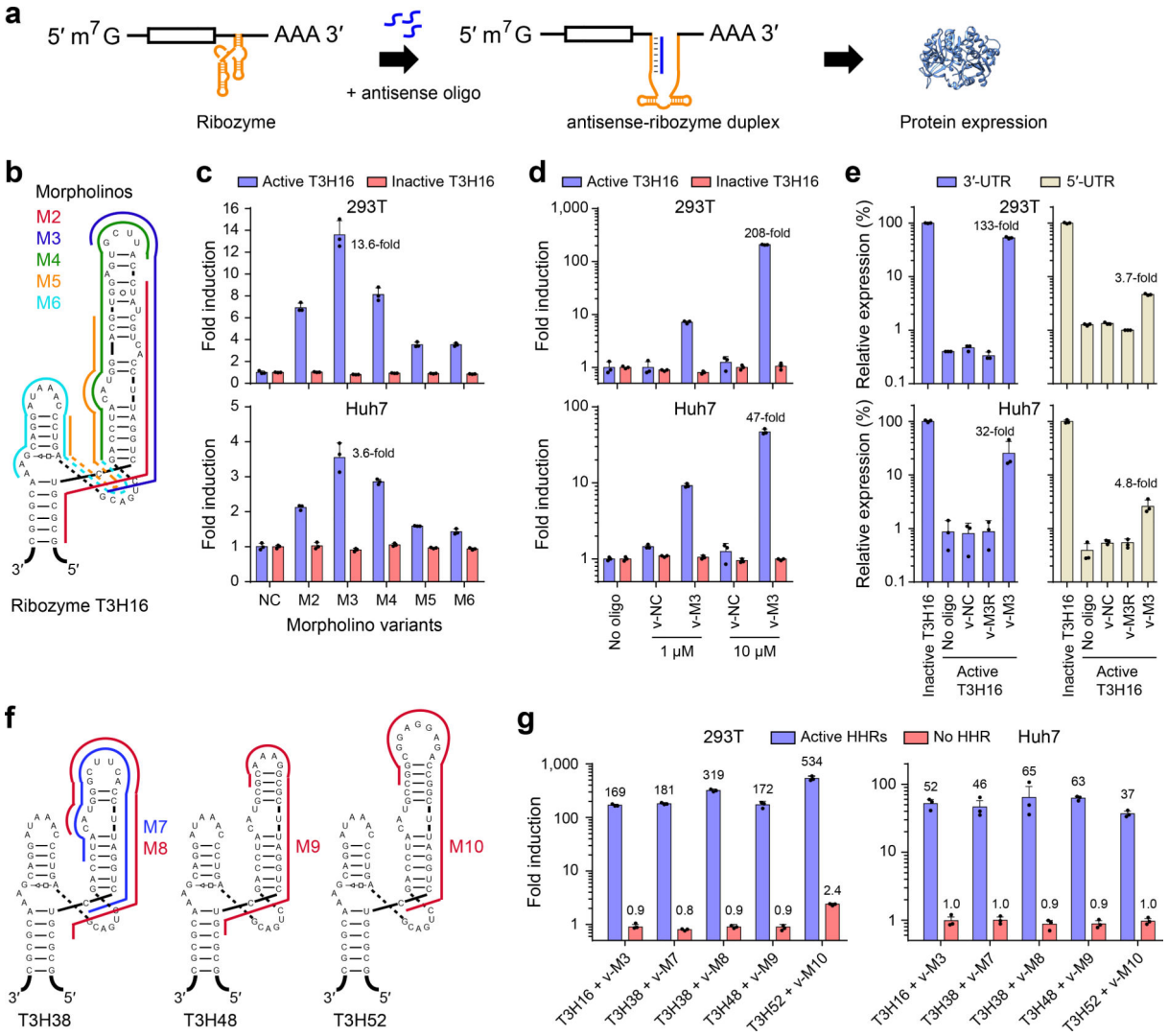

Figure 2. Efficient regulation of gene expression using optimized type III ribozymes.

(**a**) A diagram showing how an antisense oligonucleotide can inactivate a ribozyme to rescue protein expression. (**b**) The sequence and secondary structure of T3H16 ribozyme and the target regions complementary to the panel of phosphorodiamidate morpholino oligomers characterized in panel c. (**c**) 293T or Huh7 cells transfected with catalytically active or inactive T3H16 ribozyme-regulated reporter plasmids were treated with 10 μM of the indicated morpholino variants (M2 through M6) or an identical length control morpholino (NC). A functional morpholino's activity was calculated as fold induction in the Gluc reporter expression relative to the Gluc expression from the NC control morpholino-treated cells. (**d**) Experiments similar to those in panel c except that the indicated cells were treated with an octa-guanidine dendrimer-coupled form of the M3 oligo, v-M3, and a similarly coupled control oligo, v-NC. (**e**) v-M3 morpholino-mediated induction of Gluc was compared using reporter plasmids with the T3H16 ribozyme placed at 3' UTR or 5' UTR. v-M3R is randomized from the v-M3 sequence. Note that induction is significantly (two-sample *t*-test, one-sided, $P = 0.007$) greater when the ribozyme is placed at 3' UTR. (**f**) The sequences and secondary structures of three ribozyme variants, which have greater catalytic

activity than T3H16 (T3H38, T3H48) or larger stem-I loop for morpholino targeting (T3H52), and the complementary target regions of the indicated morpholinos. (**g**) Octa-guanidine dendrimer-coupled forms of morpholinos M3 and M7-M10 (v-M3, v-M7 through v-M10) were tested in 293T and Huh7 cells for induction of Gluc expression from the corresponding ribozyme variant-controlled reporter plasmid. Numbers above the figure indicate the fold induction mediated by each morpholino. Data shown are representative of two or three independent experiments with similar results, and data points represent mean ± s.d. of three cell cultures.

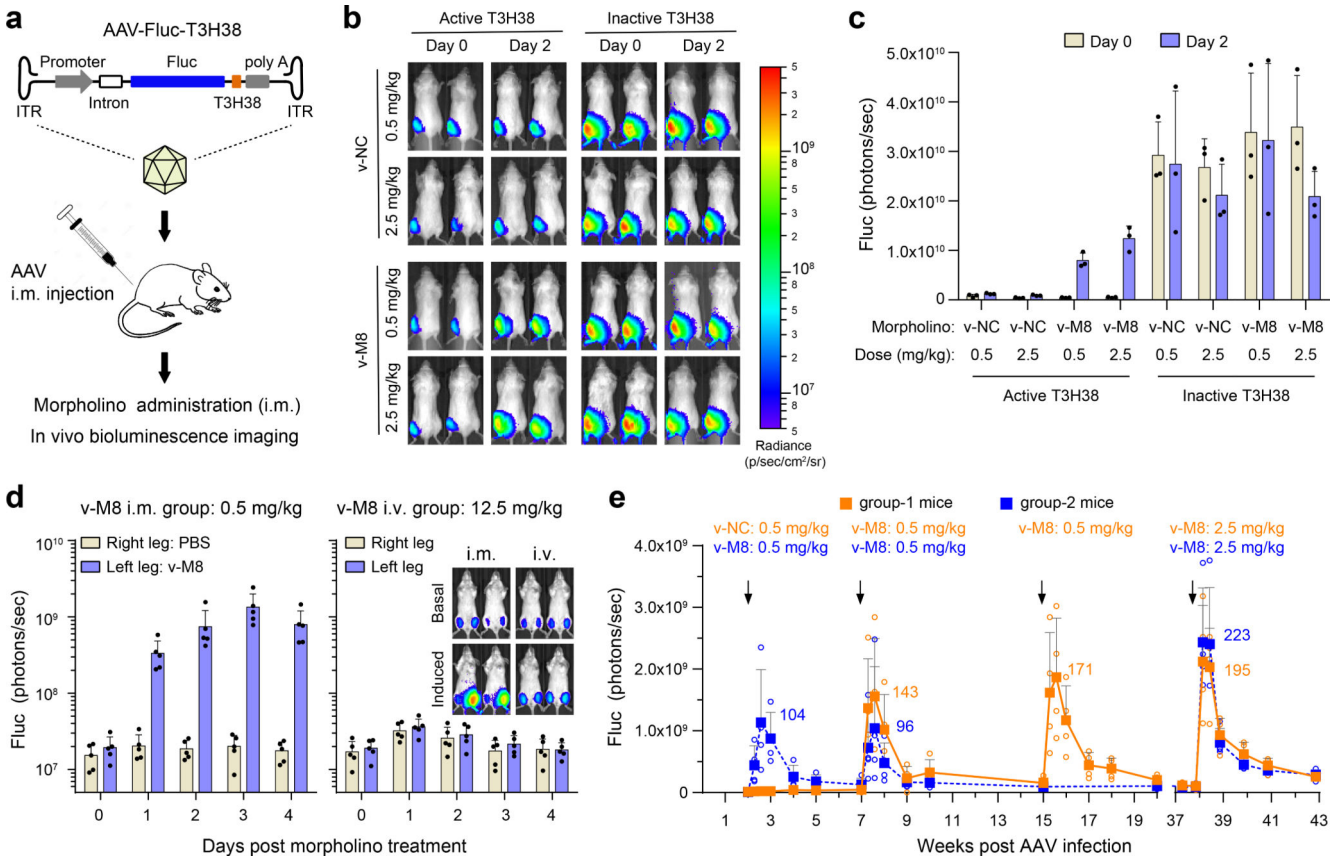

Figure 3. ***In vivo*** **induction of an adeno-associated virus (AAV) reporter transgene.**

(**a**) A diagram representing the AAV vector and the experimental design used in the animal studies of panels b through e. (**b**) Six-week old male BALB/c mice were intramuscularly (i.m.) injected in the left gastrocnemius muscle with 1×10^{10} genome copies (GC) of AAV particles carrying a T3H38-regulated firefly luciferase (Fluc) gene. Two weeks post AAV injection, mice were i.m. injected at the same site with 0.5 or 2.5 mg/kg of a control (v-NC) or the v-M8 morpholino. Bioluminescence imaging was performed at days 0 and 2 post-morpholino injection. These experiments were independently repeated three times with similar results. (**c**) Quantitation of luciferase expression shown in panel b. (**d**) An experiment similar to that shown in panel b except that 8-week old female BALB/c mice were i.m. injected at both hindlimbs with 5×10^{9} GC of T3H38-regulated AAV-Fluc. One group of mice then received an i.m. injection of 0.5 mg/kg v-M8 morpholino to one hindlimb and PBS to the other hindlimb. The other group received 12.5 mg/kg v-M8 morpholino via tail vein injection. Quantification of bioluminescence for the indicated time points is shown. Representative bioluminescent images for basal expression and induced peak expression are shown. (**e**) An experiment similar to that shown in panel b except that two groups of 8-week old female BALB/c mice were injected multiple times with the v-NC or v-M8 morpholino as indicated by the arrows. Bioluminescence imaging was performed at the indicated time points. Note that the third injection of group 2 was omitted due to a technical error. Numbers beside each peak indicate fold-induction over background measured before the first

morpholino dose. Data points in panels c, d, and e represent mean ± s.d. of three, five, and four mice per group, respectively.

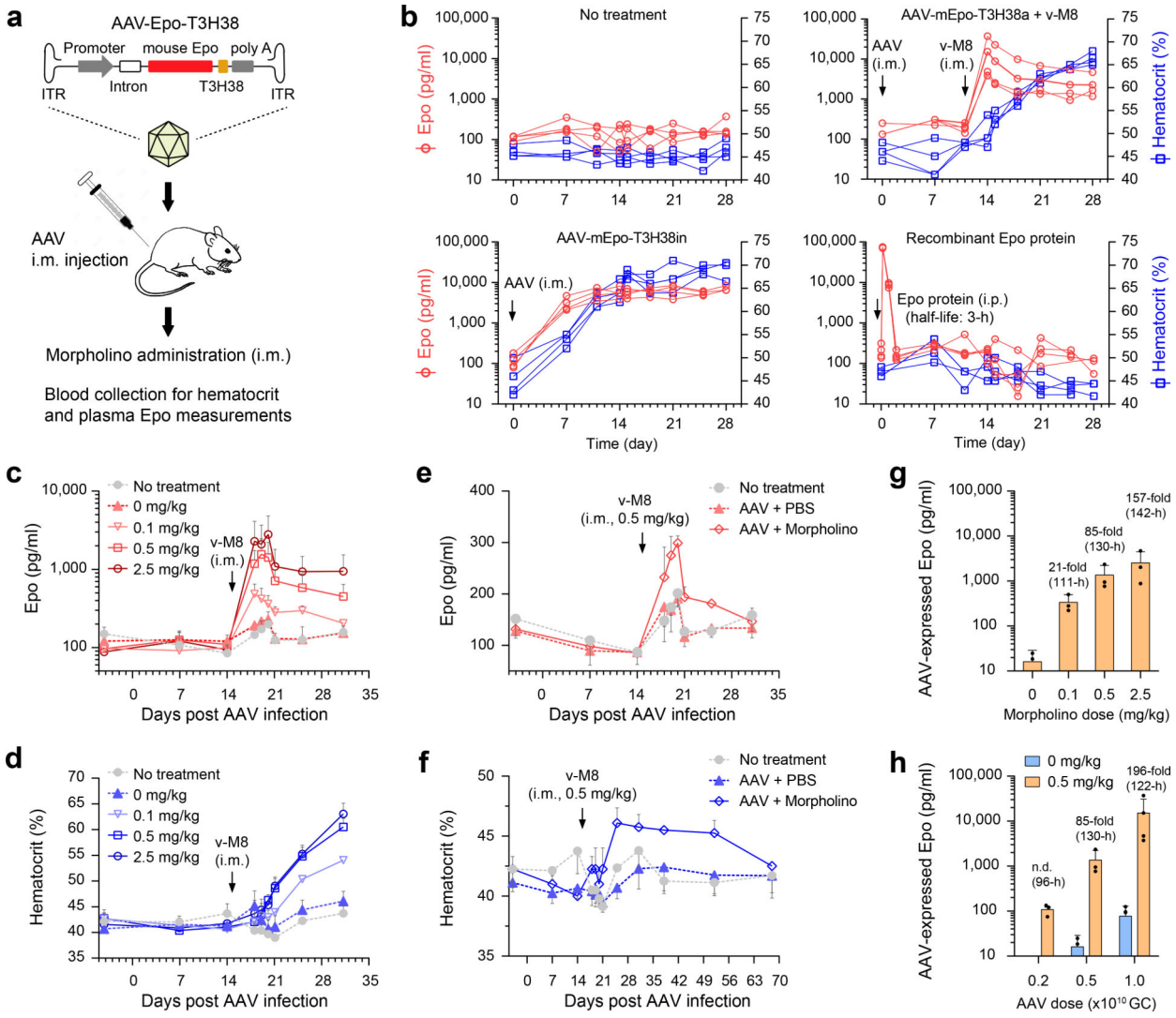

Figure 4. ***In vivo*** **regulation of an erythropoietin (Epo) transgene.**

(**a**) A diagram representing the AAV vector and the experimental design used in the following animal studies. (**b**) Eight-week old female BALB/c mice were i.m. injected with 1×10^{10} GC of AAV particles carrying an active (T3H38a; upper right panel) or inactive (T3H38in; lower left panel) T3H38-regulated mouse erythropoietin (Epo) gene. Mice injected with active ribozyme-regulated AAV were further treated with 0.5 mg/kg of the v-M8 morpholino. Mice received no treatment (upper left panel) and a group of mice intraperitoneally injected with 3 μg recombinant mouse Epo protein (lower right panel) were used as controls. Hematocrit counts (blue lines) and plasma Epo protein concentrations (red lines) were measured at the indicated time points. Each line represents values obtained from a single mouse. The morpholino induction experiments were independently repeated twice with similar results. (**c-f**) Experiments similar to panel b except that the mice were injected with 5×10^{9} GC (c and d) or 2×10^{9} GC (e and f) of AAV particles carrying active T3H38-regulated mouse Epo gene and then treated with the indicated doses of the v-M8 morpholino. All differences among sets of mice treated with different morpholino

concentrations are significant (paired-sample Student's t-test, one-sided, $P < 0.01$ for panels c, e, and f, $P < 0.05$ for panel d) except for hematocrit values at 0.5 and 2.5 mg/kg (panel d). (**g-h**) Morpholino-induced peak Epo expression data from panel c are plotted by morpholino dose (g), and data from panels b, c, and e are plotted by AAV titers (h). Endogenous Epo concentrations (150 pg/ml) have been subtracted to determine fold induction of AAV-expressed Epo. The half-life of Epo induction and induction fold are shown above the figures Data points in panels c-h represent mean ± s.d. for three mice per group.